

International Journal of Scientific Research and Reviews

Performance of a Magnetic Fluid Based Longitudinally Rough Long Bearing

Andharia P.I.^{*1}, Patel Mital² and Trivedi M.M.³

Department of Mathematics, M.K. Bhavnagar University, Bhavnagar, Gujarat, India

Email: ¹pareshandharia@yahoo.com, ²mital.kachhadia6611@gmail.com

³mmtrivedimaths@gmail.com

ABSTRACT

In this article we have studied and analysed the infinitely rough long bearing formed by a magnetic fluid as a lubricant. The magnetic field is oblique to the stator and the bearing surfaces are considered to be longitudinally rough. The roughness of the bearing surfaces is characterized by a stochastic random variable with non-zero mean, variance and skewness. The modified Reynolds' equation is stochastically averaged with respect to the random roughness parameters. It is then solved with appropriate boundary conditions to obtain the expression for pressure distribution, which is used to calculate the load carrying capacity. The results are presented graphically as well as in tabular form. Results show that the longitudinal surface roughness affects the performance of the bearing system adversely. It is seen that the load carrying capacity increases for the various values of magnetization parameter μ^* , length ratio h_2/L and standard deviation ratio σ/h_2 . It is also clearly analysed that the load carrying capacity decrease due to mean ratio α/h_2 and symmetry ratio ε/h_2 . It is revealed that the negative effect of longitudinal roughness can be minimized to certain extent by the positive effect of the magnetization. While designing the bearing system, the roughness must be given due consideration.

KEYWORDS: Long bearing, Longitudinal roughness, Magnetic fluid, Reynolds' equation

***Corresponding author**

Dr. Paresh Andharia

Assistant Professor,

Department of Mathematics, M. K. Bhavnagar University,

Bhavnagar 364 002, Gujarat, India

E-mail: pareshandharia@yahoo.com (M) 9824849825

INTRODUCTION

Purday¹ presented the case of hydrodynamic slider bearing and show that the shape of wedge is not important but the aspect ratio is important.

Hydrodynamic slider bearings are designed to maintain axial loads. Pinkus and Sternlicht² have presented the analysis of hydrodynamic lubrication. In a long bearing, the problem of negative pressure does not arise.

Infact, the infinite long slider bearing is the idealization of a single sector shaped pad of a hydrodynamic thrust bearing. Such a bearing consists of a fixed or pivoted pad and a moving pad which may be plane, stepped, curved or composite shaped. Because of the use of squeeze film slider bearing in clutch plates, automobile, transmissions and domestic appliances, many investigations (Prakash and Vij³, Bhat and Patel⁴) dealt with the problem of a squeeze film slider bearing. Slider bearing has been studied for various film shapes. (Pinkus and Sternlicht², Bagci and Singh⁵ and Hamrock⁶) as slider bearing is often used for supporting transverse loads.

In practice, bearing surfaces usually not smooth but rough. The roughness of surface is random in nature. The randomness of roughness and effect of roughness on the performance of bearing was analyzed by many investigators (Michell⁷, Davis⁸, Burton⁹, Tzeng and Saibel¹⁰, Christensen and Tonder^{11,12,13}, Tonder¹⁴, Berthe and Godet¹⁵). Following the approach of Tzeng and Saibel¹⁰, Christensen and Tonder^{11,12,13} developed a comprehensive general analysis for transverse surface roughness which was based on a general probability density function.

The method of Christensen and Tonder^{11,12,13} was deployed in many investigations to discuss the effect of surface roughness (Ting¹⁶, Prakash and Tiwari^{17,18}, Prajapati^{19,20}, Guha²¹, Gupta and Deheri²², Andharia, Gupta and Deheri^{23,24}).

All the above studies dealt with a conventional lubricant. The magnetic fluid is prepared by suspending fine magnetic grains coated with a surfactant and dispersing it in a non-conducting and magnetically passive solvent, such as benzene, hydrocarbons and fluoro carbons. These magnetic fluids remain liquid in a magnetic field and after removal of a field recover their characteristics. Particles within the liquid experience a force due to the field gradient and move through the liquid imparting drag to it causing it to flow. The advantage of magnetic fluid lubricant over the conventional ones is that the former can be retained at the desired location by an external magnetic field (Bhat²⁵).

Verma²⁶ and Agrawal²⁷ presented the squeeze film performance by taking a magnetic fluid as a lubricant. Bhat and Deheri²⁸ extended the analysis of Verma²⁶ and Agrawal²⁷ to analyse the squeeze film behaviour between porous annular disks using a magnetic fluid lubricant with the external

magnetic field oblique to the lower disk. Here, it was concluded that the application of magnetic fluid lubricant enhanced the performance of squeeze film bearing system. Subsequently, Bhat and Deheri²⁹ modified the analysis of Agrawal²⁷ by considering a magnetic fluid based porous composite slider bearing with its slider consisting of an inclined pad and a flat pad. These discussions suggested that the magnetic fluid lubricant unaltered the friction and shifted the centre of pressure towards the inlet. Moreover, the load carrying capacity registered a sharp rise due to the magnetic fluid lubricant. Bhat and Deheri³⁰ considered the hydrodynamic lubrication of a porous slider bearing and compared the performance by taking the various geometrical shapes. Here, it was observed that mostly, the magnetic fluid lubricant resulted was increased load carrying capacity and shifted the centre of pressure towards the outlet edge. Shah and Bhat³¹ extended the analysis of Ajwaliya³² to develop a mathematical model, which study the effect of slip velocity on a porous secant shaped slider bearing with ferrofluid lubricant using Jenkins model. Deheri, Andharia, Patel³³ analysed the performance of longitudinally rough slider bearing with squeeze film formed by a magnetic fluid. Here, it was shown that the magnetic fluid lubricant enhance the performance of the squeeze film bearing system. This performance was more pronounced, when suitable values of magnetization parameters were taken into the consideration. This study included the performance of a magnetic fluid based hyperbolic slider bearing. Andharia and Patel³⁴ analysed surface roughness effect of transverse patterns on the performance of short bearing. Andharia and Patel³⁵ considered longitudinally rough short bearing in their analysis. Andharia and Patel³⁶ presented performance of transversely rough long bearing. Recently Andharia³⁷ investigated performance analysis of a long bearing lubricated by a magnetic field. Here, it was observed that the load carrying capacity increase due to the magnetic fluid as lubricant.

Here, it has been proposed to study and analyse the performance of a magnetic fluid based longitudinally rough long bearing.

ANALYSIS

The geometry and configuration of bearing system which is infinite in Z -direction is shown in Figure 1, where in the slider moves with the uniform velocity U in X -direction.

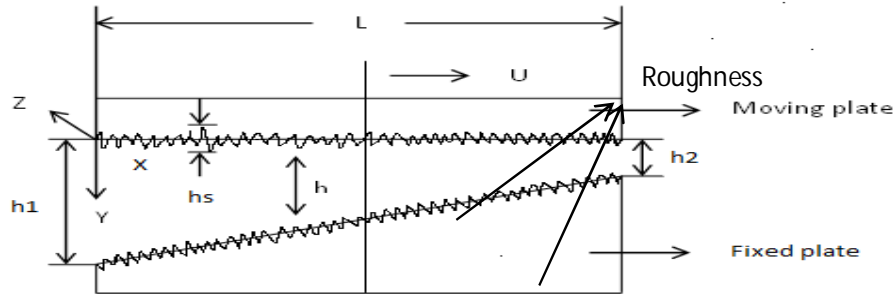


Figure 1: Bearing Configuration

The bearing surfaces are assumed to be longitudinally rough. The thickness $h(x)$ of the lubricant film is given by

$$h(x) = \bar{h}(x) + h_s \quad (1)$$

where $\bar{h}(x)$ is the mean film thickness and h_s is the deviation from the mean film thickness characterizing the random roughness of the bearing surfaces. h_s is considered to be stochastic in nature and governed by probability density function.

$$f(h_s) = \frac{35}{32C^7} (C^2 - h^2)^3, -C \leq h \leq C$$

$$= 0, \text{ elsewhere} \quad (2)$$

where C is the maximum deviation from the mean film thickness

The mean α , the standard deviation σ and the measure of symmetry ε of the random variable h_s are defined by the relationship:

$$\alpha = E(h_s), \sigma^2 = E[(h_s - \alpha)^2], \varepsilon = E[(h_s - \alpha)^3] \quad (3)$$

where E denotes the expected value defined by

$$E(R) = \int_{-C}^C f(h_s) dh_s \quad (4)$$

It is easily observed that α , σ and ε are independent of x .

The lubricant film is considered to be isoviscous and incompressible and the flow is laminar. The magnetic field is oblique to the stator as in Agrawal²⁷. The effect of various forms of the magnitude of the magnetic field been discussed as in Bhat²⁵. Thus, considering the discussions carried out therein, here the magnetic field is expressed as

$$M^2 = KL^2 \frac{x}{L} \sin\left(1 - \frac{x}{L}\right) \quad (5)$$

where K is a suitably chosen constant from dimensionless point of view (Bhat and Deheri³⁰) and L is the length of bearing.

On the basis of assumptions, the equation governing the pressure distribution in the lubricant film satisfies a modified form of Reynold's equation (Bhat²⁵, Andharia, Gupta and Deheri²³, Deheri, Andharia and Patel³³) given by

$$\frac{d}{dx} \left(p - \frac{\mu_0 \bar{\mu} M^2}{2} \right) = 6\mu u m(h)(h - \lambda h_2) \quad (6)$$

where $m(h) = h^{-3} [1 - 3\alpha h^{-1} + 6h^{-2}(\alpha^2 + \sigma^2) - 10h^{-3}(\varepsilon + 3\sigma^2\alpha + \alpha^3)]$

$$m = \frac{h_1 - h_2}{h_2}$$

$$h = h_2 \left\{ 1 + m \left(1 - \frac{x}{L} \right) \right\}$$

and $\lambda > 1$

while μ_0 is the magnetic susceptibility, $\bar{\mu}$ is the free space permeability and μ is the lubricant viscosity.

By integrating Eq. (6) with respect to x , we get the expression of pressure as

$$p = \frac{\mu_0 \bar{\mu} M^2}{2} + 6\mu u \int_0^x m(h)(h - \lambda h_2) dx \quad (7)$$

Introducing dimensionless quantities in Eq. (7)

$$\mu^* = \frac{h_2^3 k \mu_0 \bar{\mu}}{\mu u}, P = \frac{h_2^3 p}{\mu u L^2}, X = \frac{x}{L}, \bar{\alpha} = \frac{\alpha}{h_2}, \bar{\sigma} = \frac{\sigma}{h_2}, \bar{\varepsilon} = \frac{\varepsilon}{h_2^3}, H = \frac{h}{h_2}, \bar{h}_2 = \frac{h_2}{L}$$

we get the dimensionless pressure distribution as follow:

$$P = \frac{\mu^*}{2} X \cdot \sin(1 - X) + 6\bar{h}_2 \int_0^X M(H)(H - \lambda) dX \quad (8)$$

where $M(H) = m(h) h_2^3 = H^{-3} [1 - 3\alpha H^{-1} + 6H^{-2}(\alpha^2 + \sigma^2) - 10H^{-3}(\varepsilon + 3\sigma^2\alpha + \alpha^3)]$

Using associated boundary conditions

$$P = 0 \text{ at } X = 0 \text{ and } X = 1$$

in Eq. (8), we get

$$\lambda = \frac{\int_0^1 H \cdot M(H) dX}{\int_0^1 M(H) dX} \quad (9)$$

The dimensionless load carrying capacity is obtained as

$$\begin{aligned} W &= \int_0^1 P dX \\ &= 0.079265 \mu^* + 6\bar{h}_2 \int_0^1 M(H)(H - \lambda) dX \end{aligned} \quad (10)$$

where $M(H) = H^{-3} [1 - 3\alpha H^{-1} + 6H^{-2}(\alpha^2 + \sigma^2) - 10H^{-3}(\varepsilon + 3\sigma^2\alpha + \alpha^3)]$

and $H = 1 + m(1 - X)$.

RESULTS AND DISCUSSION

Eq. (8) represents the expression for the dimensionless pressure distribution and Eq. (10) determined the load carrying capacity in dimensionless form. These performance characteristics depend on various parameters such as magnetization parameter μ^* length ratio h_2/L aspect ratio m and roughness parameters σ , α and ε etc. The results are presented graphically in Figures (2) – (10) and also numerically in table form as Tables (1) – (4).

Figures (2) – (6) represent the variation of load carrying capacity with respect to magnetization parameter μ^* for various values of h_2/L , σ/h_2 , α/h_2 , ε/h_2 and m respectively. It shows that load carrying capacity increases marginally due to μ^* . These figures also indicates that the load carrying capacity increases for increasing values of h_2/L and σ/h_2 . While load capacity of the bearing decreases as α/h_2 , ε/h_2 and m increases.

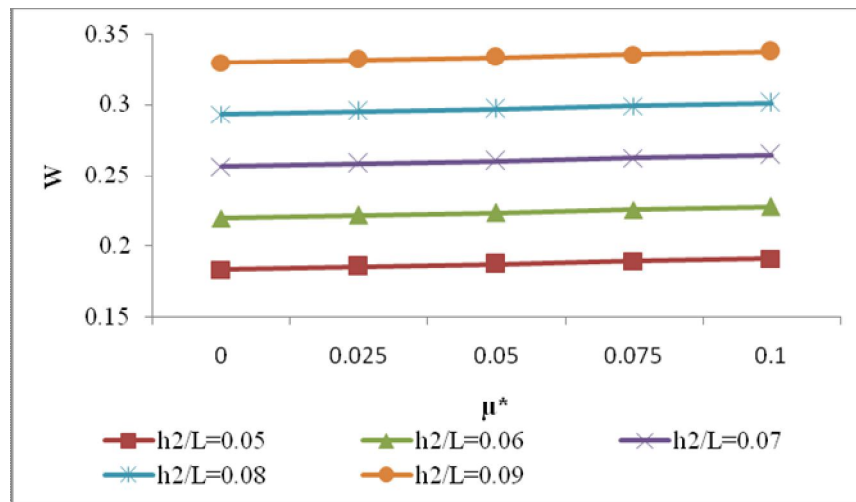


Figure 2: Variation of Load Carrying Capacity with respect to μ^* for Various h_2/L

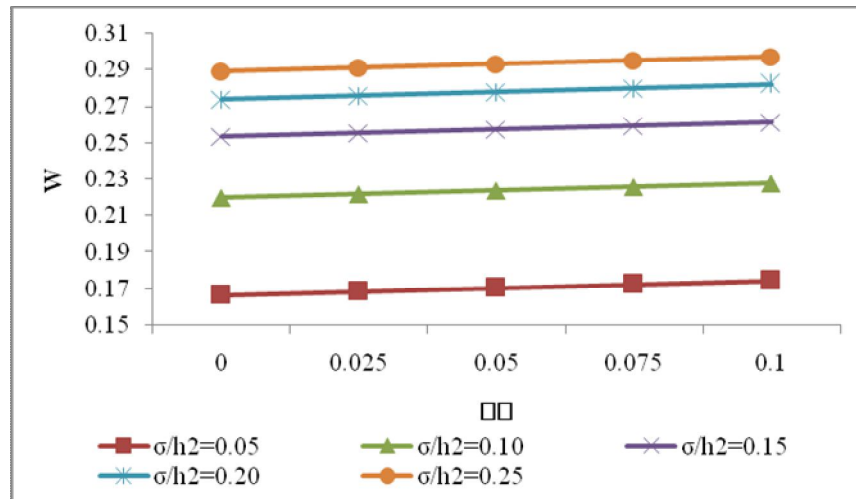


Figure 3: Variation of Load Carrying Capacity with respect to μ^* for Various σ/h_2

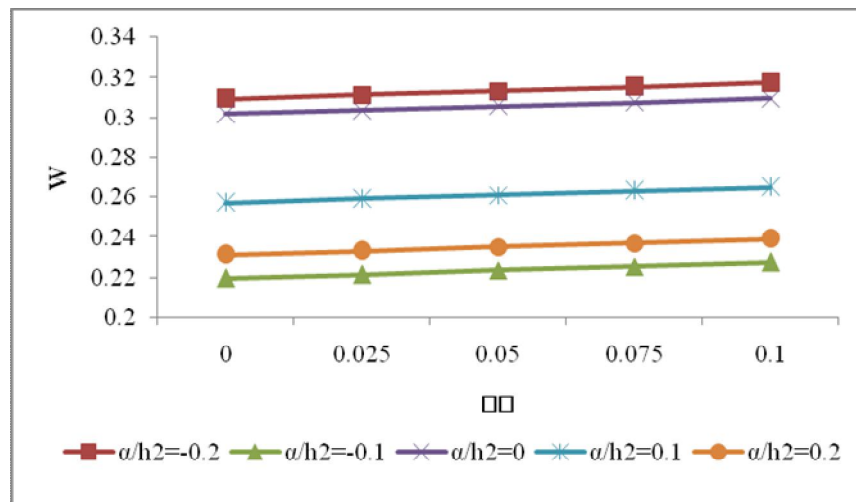


Figure 4: Variation of Load Carrying Capacity with respect to μ^* for Various a/h_2

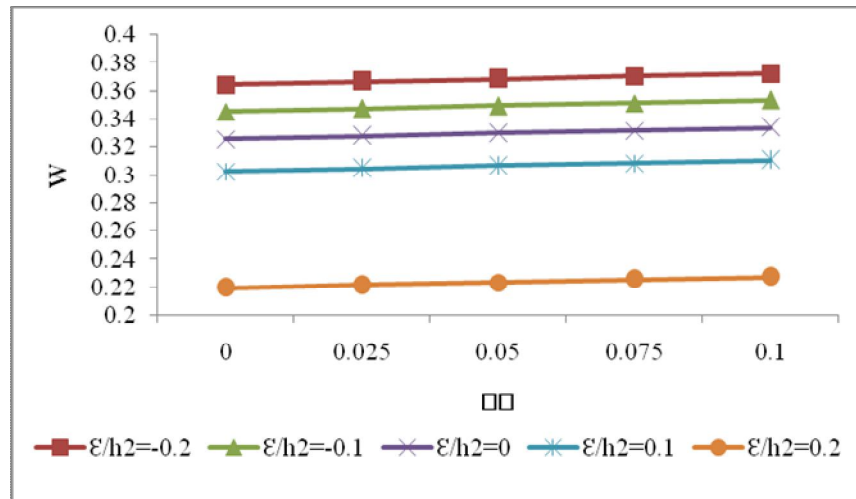


Figure 5: Variation of Load Carrying Capacity with respect to μ^* for Various ϵ/h_2

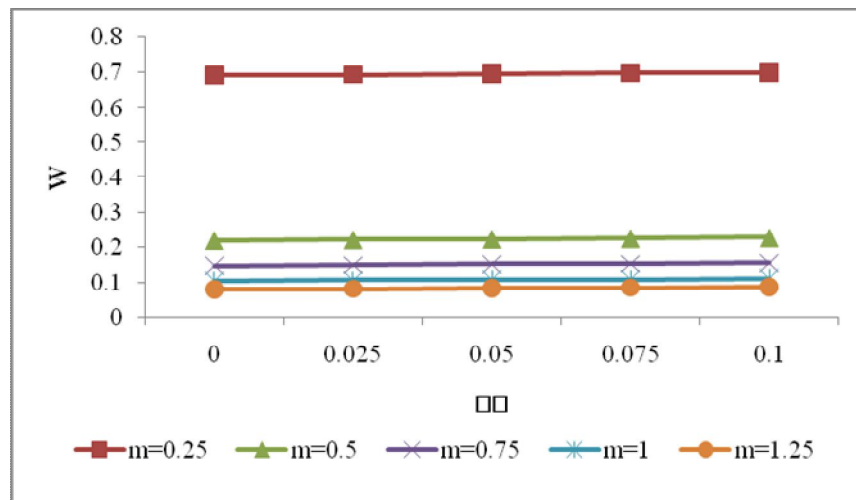


Figure 6: Variation of Load Carrying Capacity with respect to μ^* for Various m

Figures (7) – (10) show the variation of load carrying capacity with respect to h_2/L for various values of σ/h_2 , α/h_2 , ϵ/h_2 and m respectively. From these figures, it is clear that the load carrying capacity increases sharply due to h_2/L . These figures also suggest that performance of the bearing suffers in the case of α/h_2 , ϵ/h_2 and m , while it becomes better in the case of σ/h_2 .

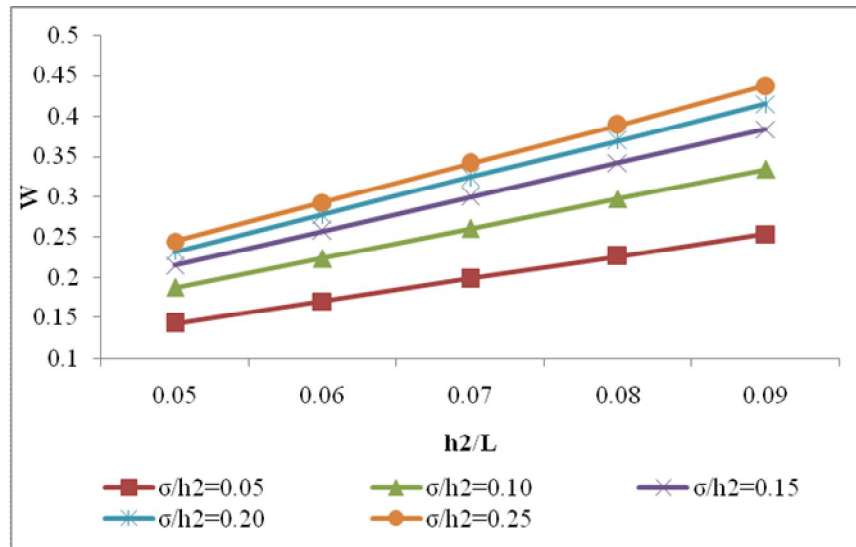


Figure 7: Variation of Load Carrying Capacity with respect to h_2/L for Various σ/h_2

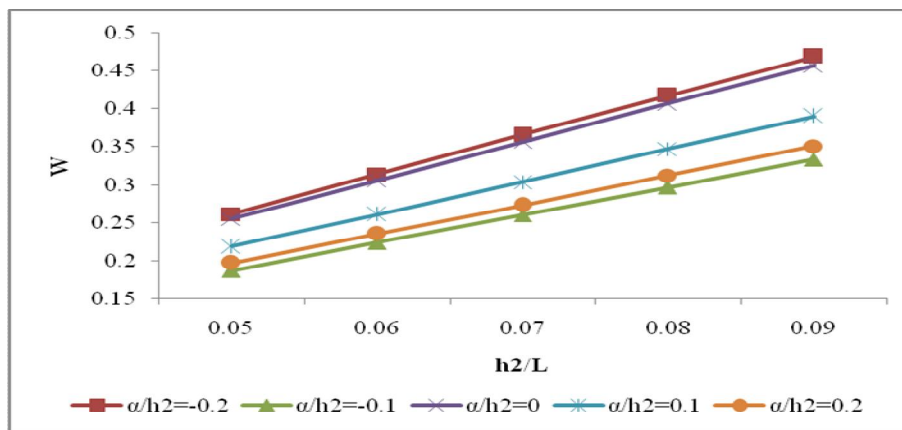


Figure 8: Variation of Load Carrying Capacity with respect to h_2/L for Various α/h_2

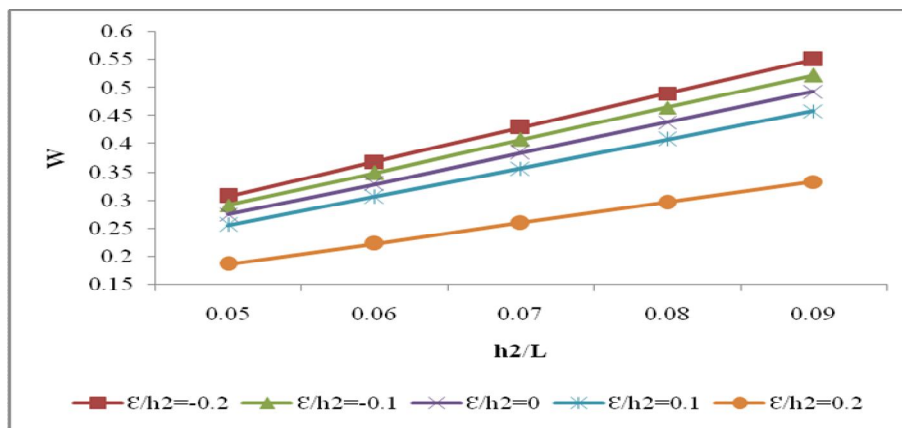


Figure 9: Variation of Load Carrying Capacity with respect to h_2/L for Various ϵ/h_2

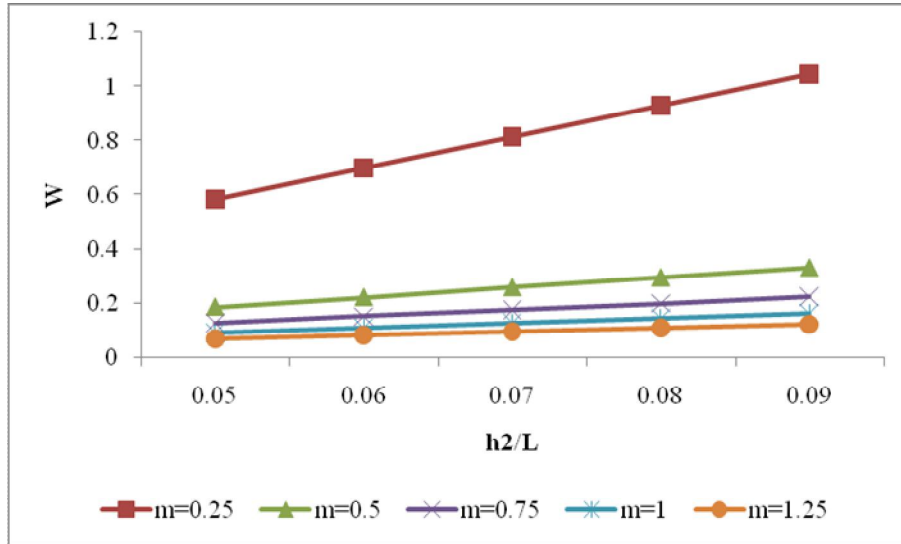


Figure 10: Variation of Load Carrying Capacity with respect to h_2/L for Various m

Tables 1 – 2 show the effect of σ/h_2 on the dimensionless load carrying capacity for various values of ε/h_2 and aspect ratio m respectively. It shows that the load carrying capacity increases significantly due to σ/h_2 and decreases for increasing values of ε/h_2 and m . Table – 3 presents the effect of α/h_2 on the dimensionless load carrying capacity for various values of ε/h_2 . It is seen that the load capacity decrease marginally for the increasing values of ε/h_2 . Table – 4 suggests that the ratios ε/h_2 and m both adversely affect on the performance of the bearing.

Table 1: “Variation of Load Carrying Capacity with respect to σ/h_2 and ε/h_2 ”

σ/h_2	$\varepsilon/h_2=-0.2$	$\varepsilon/h_2=-0.1$	$\varepsilon/h_2=0$	$\varepsilon/h_2=0.1$	$\varepsilon/h_2=0.2$
0.05	0.366469	0.347674	0.327839	0.304153	0.170486
0.1	0.36845	0.349686	0.329946	0.306755	0.22366
0.15	0.371752	0.353035	0.333435	0.310928	0.257149
0.2	0.37637	0.357713	0.338283	0.316515	0.277839
0.25	0.382303	0.363713	0.344463	0.323393	0.292758

Table 2: “Variation of Load Carrying Capacity with respect to σ/h_2 and m ”

σ/h_2	$m=0.25$	$m=0.5$	$m=0.75$	$m=1$	$m=1.25$
0.05	0.667339	0.170486	0.142125	0.104469	0.080751
0.1	0.697641	0.22366	0.152078	0.109609	0.084151
0.15	1.92298	0.257149	0.163065	0.116003	0.088594
0.2	0.592779	0.277839	0.172957	0.122386	0.093237
0.25	0.639325	0.292758	0.181587	0.128325	0.097692

Table 3: “Variation of Load Carrying Capacity with respect to α/h_2 and ε/h_2 ”

α/h_2	$\varepsilon/h_2=-0.2$	$\varepsilon/h_2=-0.1$	$\varepsilon/h_2=0$	$\varepsilon/h_2=0.1$	$\varepsilon/h_2=0.2$
-0.2	0.401197	0.382523	0.363176	0.34209	0.313448
-0.1	0.36845	0.349686	0.329946	0.306755	0.22366
0	0.340989	0.322188	0.302066	0.274698	0.305727
0.1	0.317702	0.298913	0.278438	0.239007	0.261047
0.2	0.297473	0.278713	0.257822	1.70953	0.235113

Table 4: “Variation of Load Carrying Capacity with respect to ε/h_2 and m ”

ε/h_2	$m=0.25$	$m=0.5$	$m=0.75$	$m=1$	$m=1.25$
-0.2	0.817775	0.36845	0.227241	0.160191	0.121733
-0.1	0.769407	0.349686	0.216728	0.153264	0.116736
0	0.720212	0.329946	0.205278	0.145488	0.110985
0.1	0.66735	0.306755	0.190898	0.135247	0.103143
0.2	0.697641	0.22366	0.152078	0.109609	0.084151

CONCLUSION

This investigation establishes that the performance of the bearing system can be improved considerably by choosing appropriate values of the standard deviation, aspect ratio and the outlet thickness ratio. These three parameters can be responsible for better performance for the magnetic fluid based longitudinally rough long bearing.

REFERENCES

1. Purday HFP. Streamline Flow. Constable and Co.: London; 1949.
2. Pinkus O, Stemlicht B. Theory of Hydrodynamic Lubrication. McGraw-Hill Book Company: New York; 1961.
3. Prakash J, Vij SK. Hydrodynamic lubrication of a porous slider. Journal of Mechanical Engineering and Science. 1973; 15: 222-234.
4. Bhat MV, Patel CM. The squeeze film in an inclined porous slider bearing. WEAR. 1981; 66: 189-193.
5. Bagci C, Singh AP. Hydrodynamic lubrication of a finite slider bearing, effect of one dimensional film shape and their computer aided optimum designs. Journal of Lubrication and Technology, ASLE Transaction. 1983; 105: 48-66.
6. Hamrock BJ. Fundamentals of fluid film lubrication. McGraw Hill Book Company: New York; 1994.
7. Michell AGM. Lubrication: Its principles and practice. Blackie and Son Limited: London; 1950.
8. Davis MG. The generation of pressure between rough fluid lubricated moving deformable surfaces. Lubrication of Engineering. 1963; 19: 246.
9. Burton RA. Effect of two dimensional sinusoidal roughness on the load support characteristics of a lubricant film. Journal of Basic Engineering, Transaction of ASME. 1963; 85: 258-264.
10. Tzeng ST, Saibel E. Surface roughness effect on slider bearing lubrication. Journal of Lubrication and Technology, Transaction of ASME. 1967; 10: 334-338.
11. Christensen H, Tonder KC. Tribology of rough surfaces: Stochastic models of hydrodynamic lubrication. SINTEF Report. 1969; No. 10/69-18.
12. Christensen H, Tonder KC. Tribology of rough surfaces: parametric study and comparison of lubrication models. SINTEF Report. 1969; No. 22/69-18.
13. Christensen H, Tonder KC. The hydrodynamic lubrication of rough bearing surfaces of finite width. ASME-ASLE Lubrication Conference, Cincinnati, Ohio. 1970; Paper No.70, Lub-7.

14. Tonder KC. Surface distributed waviness and roughness. Proc. First World Conference in Industrial Tribology, New-Delhi (India). 1972; 3A: 01-08.
15. Berthe D, Godet M. A More general form of Reynolds equation – application to rough surfaces. WEAR. 1973; 27: 345-357.
16. Ting LL. Engagement behaviour of lubricated porous annular disks Part-1: Squeeze film phase, surface roughness and elastic deformation effects. WEAR. 1975; 34: 159-182.
17. Prakash J, Tiwari K. Lubrication of porous bearing with surface corrugations. Journal of Lubrication and Technology, Transaction ASME. 1982; 104: 127-134.
18. Prakash J, Tiwari K. Roughness effect in porous circular squeeze plate with arbitrary wall thickness. Journal of Lubrication and Technology, Transaction ASME. 1983; 105: 90-95.
19. Prajapati BL. Behaviour of squeeze film between rotating porous circular plates: Surface roughness and elastic deformation effects. Pure and Applied Mathematical Science. 1991; 33: 27-36.
20. Prajapati BL. Behaviour of squeeze film between rotating porous circular plates with a concentric circular pocket: Surface roughness and elastic deformation effects. WEAR. 1992; 152: 301-307.
21. Guha SK. Analysis of dynamic characteristics of hydrodynamic journal bearing with isotropic roughness effect. WEAR. 1993; 167: 173-179.
22. Gupta JL, Deheri GM. Effects of roughness on the behaviour of squeeze film in a spherical bearing. Tribology Transactions. 1996; 39: 99-102.
23. Andharia PI, Gupta JL, Deheri GM. Effects of longitudinal surface roughness on hydrodynamic lubrication of slider bearing. Proc. Tenth International conference on surface modification Technologies, The Institute of materials, London. 1997; 872-880.
24. Andharia PI, Gupta JL, Deheri GM. Effects of transverse surface roughness on the behaviour of squeeze film in a spherical bearing. Journal of Applied Mechanics and Engineering. 1999; 4: 19-24.
25. Bhat MV. Lubrication with a magnetic fluid. Teamspirit (India) Pvt. Ltd.; 2003.
26. Verma PDS. Magnetic fluid based squeeze film. International Journal of Engineering Science. 1986; 24: 395-401.
27. Agrawal VK. Magnetic fluid based porous inclined slider bearing. WEAR. 1986; 107: 133-139.
28. Bhat MV, Deheri GM. Squeeze film behaviour in porous annular discs lubricated with magnetic fluid. WEAR. 1991; 151: 123-128.

29. Bhat MV, Deheri GM. Porous composite slider bearing lubricated with magnetic fluid. Japanese Journal of Applied Physics. 1991; 30: 2513-2514.
 30. Bhat MV, Deheri GM. Porous slider bearing with squeeze film formed by a magnetic fluid. Pure and Applied Mathematical Sciences. 1995; 39: 39-43.
 31. Shah RC, Bhat MV. Effect of slip velocity in a porous secant shaped slider bearing with a Ferrofluid lubricant. FIZIKAA. 2003; 12: 1-8.
 32. Ajwaliya MB. Hydrodynamic lubrication of a secant shaped porous slider, Thesis, SP University, India. 1984.
 33. Deheri GM, Andharia PI, Patel RM. Transversely rough slider bearing with squeeze film formed by a magnetic fluid. International Journal of Applied Mechanics and Engineering. 2005; 10: 53-76.
 34. Andharia PI, Patel M. The Surface Roughness Effect of Transverse Patterns on the Performance of Short Bearing. International Journal of Scientific & Engineering Research, 2015; 6: 82-87.
 35. Andharia PI, Patel M. Longitudinally Rough Short Bearing. International Journal of Science and Research, 2015; 4: 2497-2502.
 36. Andharia PI, Patel M. Performance of a Transversely Rough Long Bearing. Journal of Environmental Science, Computer Science and Engineering & Technology. 2017; Sec. C, 6(4): 511-522.
 37. Andharia PI. Performance analysis of a long bearing lubricated by a magnetic field. International Journal of Computer & Mathematical Science. 2018; 7(3): 13-19.
-